

Division accuracy in a stochastic model of Min oscillations in *Escherichia coli*

Rex A. Kerr^{*†‡}, Herbert Levine^{†§}, Terrence J. Sejnowski^{*†¶}, and Wouter-Jan Rappel^{†§}

^{*}Computational Neurobiology Laboratory and [¶]Howard Hughes Medical Institute, The Salk Institute for Biological Studies, La Jolla, CA 92037; and [†]Center for Theoretical Biological Physics, [§]Department of Physics, [¶]Division of Biological Sciences, University of California, San Diego, La Jolla, CA 92093

Edited by Harry L. Swinney, University of Texas, Austin, TX, and approved November 7, 2005 (received for review July 11, 2005)

Accurate cell division in *Escherichia coli* requires the Min proteins MinC, MinD, and MinE as well as the presence of nucleoids. MinD and MinE exhibit spatial oscillations, moving from pole to pole of the bacterium, resulting in an average MinD concentration that is low at the center of the cell and high at the poles. This concentration minimum is thought to signal the site of cell division. Deterministic models of the Min oscillations reproduce many observed features of the system, including the concentration minimum of MinD. However, there are only a few thousand Min proteins in a bacterium, so stochastic effects are likely to play an important role. Here, we show that Monte Carlo simulations with a large number of proteins agree well with the results from a deterministic treatment of the equations. The location of minimum local MinD concentration is too variable to account for cell division accuracy in wild-type, but is consistent with the accuracy of cell division in cells without nucleoids. This finding confirms the need to include additional mechanisms, such as reciprocal interactions with the cell division ring or positioning of the nucleoids, to explain wild-type accuracy.

dynamics | MCELL | FtsZ

The rod-shaped bacterium *Escherichia coli* reproduces by elongating along its long axis, duplicating its genetic material, and dividing symmetrically into two daughter cells. Wild-type *E. coli* locates the plane of cell division at 0.5 ± 0.013 of the distance along the long axis of the cell (1). This accuracy is surprising given that the cell apparently relies on the collective action of individual molecules that are a few nanometers long to measure the center of a cell that is a few microns long.

A variety of proteins are known to be involved in cell division in *E. coli*. In particular, cell division is implemented mechanically by a contractile ring formed predominantly by the FtsZ protein (2); the location of the FtsZ ring determines the site of cell division. During cell division, the bacterial chromosomes for the daughter cells are collected into two nucleoids that segregate to either side of the cell (3, 4) and fill much of the interior of the cell. Formation of the FtsZ ring is inhibited by the presence of the nucleoids (1, 5), leaving three bands in which to place the FtsZ ring: either pole or the center. The Min proteins are required for selection of the central band and precise positioning within the central band (1). MinC inhibits formation of the FtsZ ring, whereas MinD appears to recruit MinC (reviewed in ref. 6). These proteins show dynamic changes in localization throughout the cell (7–9). In particular, MinD oscillates from end to end of the cell with a period of ≈ 40 s (7); averaged over many cycles, MinD is at a higher concentration at the ends of the cell than in the center. Another protein, MinE, forms moving bands inside the cell and is required for MinD oscillations (10, 11). Thus, dynamic oscillations of MinD and MinE set up a concentration minimum of MinD at the center of the cell, leading to a low concentration of MinC at the center and enabling FtsZ ring formation at the cell's midpoint but not at its poles (12). Of the two mechanisms required for accurate cell division, the Min system seems more important: in mutants missing MinC, MinD, and MinE, placement of the plane of cell division is not restricted

to three tightly defined nucleoid-free regions, but rather is broadly distributed (1). In nucleoid-free cells, the division apparatus still assembles near the center of the cell, but with a reduced accuracy of ± 0.062 rather than ± 0.013 cell lengths (1, 5).

Because of the importance of the Min system and the unexpected dynamics of the proteins, a variety of models of Min oscillations have been developed by using deterministic (13–18) or stochastic methods (19). These models reproduce many of the features of the biological system, including a concentration minimum of MinD at the center of the cell. Deterministic models of Min oscillations assume that there are a sufficiently large number of proteins to treat their concentrations as continuous variables. However, there are only a few thousand Min proteins in an *E. coli* cell (20, 21). If MinD proteins were stationary, the cell would have to position the FtsZ ring on the basis of only tens of Min molecules locally. Oscillations provide an opportunity for the cell to take multiple independent samples of Min concentration, but it is not immediately apparent whether this temporal averaging is sufficient to allow accurate midpoint determination. Therefore, we asked whether, in the context of current models, the observed accuracy of cell division could be achieved by simply selecting the site at which the local MinD concentration is lowest.

To answer this question, we constructed a stochastic simulation of Min oscillations based on the reaction–diffusion scheme of Huang *et al.* (16, 22). This scheme was an attractive choice for three reasons. First, a deterministic analysis of the scheme reproduces many features of the biological oscillations quite well. Second, the scheme is based in biologically realistic interactions. Third, the scheme is of a form that is immediately suitable for simulation in the stochastic modeling program MCELL (23, 24). Using MCELL, we reproduced the results of the deterministic analysis for a large number of molecules and demonstrated robust oscillations that can be disrupted by decreasing the number of Min proteins in the cell. In addition, we have examined the accuracy with which the cell could determine its midpoint if it made its decision based solely on finding the minimum local MinD concentration. The scheme can account for the accuracy of cells without nucleoids, but fails to reproduce the accuracy of wild-type cells.

Methods

Monte Carlo Modeling of Min Oscillations. MCELL is a Monte Carlo modeling program for cellular microphysiology. It has been described in detail elsewhere (23) and has been validated extensively. In brief, it represents cell membranes and other boundaries as arbitrary triangulated surfaces specified by the user, and represents each molecule as a point diffusing within

Conflict of interest statement: No conflicts declared.

This paper was submitted directly (Track II) to the PNAS office.

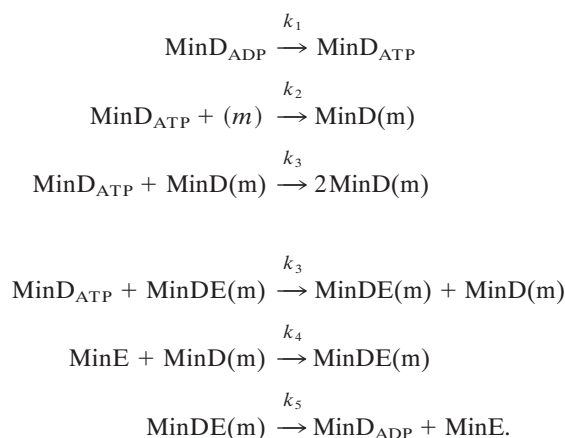
Abbreviations: D/E, MinD/MinE ratio; CV, coefficient of variation.

[†]To whom correspondence should be addressed. E-mail: kerr@salk.edu.

© 2005 by The National Academy of Sciences of the USA

those boundaries. Each molecule diffuses stochastically by picking a distance and direction of motion consistent with diffusion of a point source over some short time step, and travels in a straight line to reach that endpoint. A moving molecule reflects when its path intersects an impermeable surface element, and reacts stochastically when its path intersects another molecule. The probability of each reaction is set by specifying a bulk rate constant, which is then internally converted into the appropriate probability of reaction per collision. A stochastic MCELL model consists of a series of chemical reactions specifying the rates of reaction, the diffusion constants for the diffusing molecular species, and a model geometry. We used a new version of MCELL that allows variable-length time steps; for our models of Min oscillations, this reduced the run time of the simulations by an order of magnitude.

The Huang *et al.* scheme (16) uses a series of chemical reactions (illustrated in Fig. 1A)



Here, (m) alone refers to a patch of membrane without anything bound to it, and (m) after the name of a molecular species indicates that the molecule is bound to the membrane. This series of chemical reactions, in contrast to the systems of equations used in other Min system models (13–15), is immediately suitable for simulation using MCELL. Each patch of membrane can be occupied by at most one molecule, so the self-aggregation reactions with rate k_3 require searching for a free patch of membrane for the new MinD(m) molecule. Because the deterministic equations do not include a term for depletion of binding sites, we used a fairly large value for the search radius (50–100 nm). Moderate changes to this value did not significantly change our results (data not shown). The values used for the reaction rates are given in Table 1. In the default simulations with 5,400 proteins, there were 4,000 membrane-binding sites per μm^2 . The diffusion constants for MinD_{ADP} , MinD_{ATP} , and MinE were $2.5 \mu\text{m}^2/\text{s}$. Membrane-bound molecules were not allowed to diffuse.

Model Geometry. We created a simple 20-sided polyhedral cylinder of $4\text{-}\mu\text{m}$ length with a $0.5\text{-}\mu\text{m}$ radius, as shown in Fig. 1B. For computational efficiency, we also created a model geometry consisting of a $4\text{-}\mu\text{m}$ -long rectangular box with sides of length $\sqrt{\pi}/2$, preserving the volume of the model cell, and decreased the rate constant k_2 for the side walls by a factor of $\sqrt{\pi}/2$ to account for the increased surface area and hence increased number of binding sites. By default, the model was populated with 5,400 molecules, as in ref. 16, with varying ratios of MinD to MinE. Initially, all MinE molecules were placed along the central axis $0.25 \mu\text{m}$ from one pole of the cell, and all MinD molecules were placed in ADP-bound form $0.25 \mu\text{m}$ from the opposite pole. To compare simulation results with experimental results, we ran all simulations for 20 min of simulated time

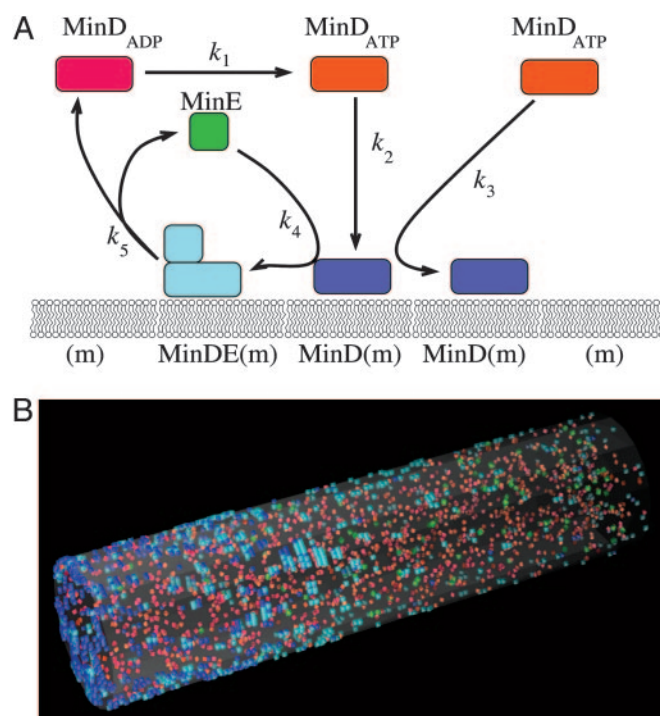


Fig. 1. Reactions and geometry of the stochastic Min oscillation model. (A) Reaction cycle. Cytosolic MinD in its ADP-bound form converts to an ATP-bound form with rate k_1 . MinD-ATP binds to the membrane alone with rate k_2 , and membrane-bound MinD (with or without MinE) catalyzes its own addition to the membrane at rate k_3 . Cytosolic MinD binds membrane-bound MinD with rate k_4 . Finally, the MinE/MinD complex dephosphorylates and dissociates into cytosolic MinE and MinD-ADP at rate k_5 . (B) Snapshot of a simulation running inside a $4\text{-}\mu\text{m}$ -long, $0.5\text{-}\mu\text{m}$ -radius triangulated cylinder (transparent surface) after 3 min of simulated time. Each colored dot is a single molecule. Colors for each state are from A. There are 5,400 proteins and a MinD/MinE ratio of 4.0.

(approximately one cell division cycle in exponential growth phase); this represents the maximum time a cell has to measure MinD concentrations. We did not change the cell length during the simulation.

Deterministic Modeling of Min Oscillations. To compare the results from our stochastic simulations with deterministic solutions of the reaction scheme, we numerically integrated the equations of ref. 16, along with its parameter values, using a simple explicit time-stepping routine. Space was discretized by using a cubic (for the box geometry) or cylindrical (for the cylinder) grid with a grid spacing of $0.05\text{--}0.1 \mu\text{m}$. We verified that a smaller grid spacing did not change the results appreciably (data not shown).

Measurement of Concentration and Oscillation Period. The local concentrations of Min proteins were determined by dividing the model cell into $n_b = 800$ bins of equal width along its long axis. The number of proteins in each bin was converted into a concentration, with a concentration of $2.7 \mu\text{M}$ corresponding to

Table 1. Reaction rates for the stochastic Min model in cylindrical geometry

Variable	k_1	k_2	k_3	k_4	k_5
Value	1.0	3.8×10^4	9.0×10^5	5.6×10^7	0.7
Units	s^{-1}	$\text{M}^{-1} \cdot \text{s}^{-1}$	$\text{M}^{-1} \cdot \text{s}^{-1}$	$\text{M}^{-1} \cdot \text{s}^{-1}$	s^{-1}

straints that are not captured by the simple model of MinD recruitment used here. For example, a model of MinD coils that alternately grow from opposite ends of the cell, as suggested in ref. 28, might result in a markedly steeper dip in MinD concentration, allowing greater accuracy. Alternatively, the interaction between MinD and the FtsZ ring may not be one-way. Models incorporating mutual antagonism between FtsZ ring formation and MinD coil formation may lead to a central FtsZ ring that is pushed from side to side by each wave of MinD, but which also prevents MinD from crossing. The nucleoids could then simply be responsible for starting the FtsZ ring in a reasonable range. Interaction dynamics such as these, if they exist, may be visible experimentally in bacteria expressing cyan and yellow fluorescent protein-labeled MinD and FtsZ.

Another possibility is motivated by noticing that the simulated reaction scheme we used for the Min signaling system is consistent with experiments that show that anucleated cells, obviously lacking the occlusion mechanism, display a greatly reduced cell division accuracy (1, 5). In fact, over a wide range of model parameters, the division accuracy obtained in our stochastic simulations is comparable to the accuracy obtained in these experiments (see Fig. 4D). This finding suggests that our model may capture the essential stochastic features of the Min system but needs to be expanded with a description of the nucleoid occlusion mechanism.

How might this nucleoid occlusion mechanism function? Our results indicate that this mechanism should not merely restrict the possible FtsZ ring formation sites but should be actively involved in midpoint determination. Further evidence for such an active role comes from experiments showing that cells missing the Min proteins have abnormally localized nucleoids (29). Perhaps the Min system has a twofold effect on cell division accuracy: a direct effect on FtsZ localization, transduced by MinC and based on local MinD concentration; and an indirect effect where MinD concentration acts to properly structure and position the nucleoids over a relatively long integration time, and nucleoid exclusion refines the position of the FtsZ ring. This model is appealing because it suggests a physical mechanism for averaging MinD concentration over a large fraction of the cell, which, as we have shown, can improve accuracy to the needed level.

We thank Dr. Thomas Bartol, Jr., for assistance with and advice on computational methods for stochastic modeling and 3D visualization of data. This work was supported by the National Science Foundation Physics Frontier Center-sponsored Center for Theoretical Biological Physics (Grants PHY-0216576 and PHY-0225630). Additional support was provided by National Institutes of Health Grant T32 0007220 (to R.A.K.) and the Howard Hughes Medical Institute (T.J.S.).

1. Yu, X.-C. & Margolin, W. (1999) *Mol. Microbiol.* **32**, 315–326.
2. Lutkenhaus, J. (1993) *Mol. Microbiol.* **9**, 403–409.
3. Valkenburg, J. A. C., Woldringh, C. L., Brakenhoff, G. J., van der Voort, H. T. M. & Nanninga, N. (1985) *J. Bacteriol.* **161**, 478–483.
4. Zimmerman, S. B. (2002) *J. Struct. Biol.* **142**, 256–265.
5. Sun, Q., Yu, X.-C. & Margolin, W. (1998) *Mol. Microbiol.* **29**, 491–503.
6. Lutkenhaus, J. (2002) *Curr. Opin. Microbiol.* **5**, 548–552.
7. Raskin, D. M. & de Boer, P. A. J. (1999) *Proc. Natl. Acad. Sci. USA* **96**, 4971–4976.
8. Hu, Z. & Lutkenhaus, J. (1999) *Mol. Microbiol.* **34**, 82–90.
9. Raskin, D. M. & de Boer, P. A. J. (1999) *J. Bacteriol.* **181**, 6419–6424.
10. Fu, X., Shih, Y.-L., Zhang, Y. & Rothfield, L. I. (2001) *Proc. Natl. Acad. Sci. USA* **98**, 980–985.
11. Hale, C. A., Meinhardt, H. & de Boer, P. A. J. (2001) *EMBO J.* **20**, 1563–1572.
12. Margolin, W. (2001) *Curr. Biol.* **11**, R395–R398.
13. Meinhardt, H. & de Boer, P. A. J. (2001) *Proc. Natl. Acad. Sci. USA* **98**, 14202–14207.
14. Howard, M., Rutenberg, A. D. & de Vet, S. (2001) *Phys. Rev. Lett.* **87**, 278102.
15. Kruse, K. (2002) *Biophys. J.* **82**, 618–627.
16. Huang, K. C., Meir, Y. & Wingreen, N. S. (2003) *Proc. Natl. Acad. Sci. USA* **100**, 12724–12728.
17. Meacci, G. & Kruse, K. (2005) *Phys. Biol.* **2**, 89–97.
18. Drew, D. A., Osborn, M. J. & Rothfield, L. I. (2005) *Proc. Natl. Acad. Sci. USA* **102**, 6114–6118.
19. Howard, M. & Rutenberg, A. D. (2003) *Phys. Rev. Lett.* **90**, 128102.
20. Zhao, C.-R., de Boer, P. A. & Rothfield, L. I. (1995) *Proc. Natl. Acad. Sci. USA* **92**, 4313–4317.
21. Shih, Y.-L., Fu, X., King, G. F., Le, T. & Rothfield, L. (2002) *EMBO J.* **21**, 3347–3357.
22. Kulkarni, R. V., Huang, K. C., Kloster, M. & Wingreen, N. S. (2004) *Phys. Rev. Lett.* **93**, 228103.
23. Stiles, J. R. & Bartol, T. M. (2001) in *Computational Neurobiology: Realistic Modeling for Experimentalists*, ed. de Schutter, E. (CRC Press, Boca Raton, FL), pp. 87–127.
24. Coggan, J. S., Bartol, T. M., Esquenazi, E., Stiles, J. R., Lamont, S., Martone, M. E., Berg, D. K., Ellisman, M. H. & Sejnowski, T. J. (2005) *Science* **309**, 446–451.
25. Anderson, D. E., Guieros-Filho, F. J. & Erikson, H. P. (2004) *J. Bacteriol.* **186**, 5775–5781.
26. Chen, Y. & Erickson, H. P. (2005) *J. Biol. Chem.* **280**, 22549–22554.
27. Suefujii, K., Valluzzi, R. & RayChaudhuri, D. (2002) *Proc. Natl. Acad. Sci. USA* **99**, 16776–16781.
28. Shih, Y.-L., Le, T. & Rothfield, L. (2003) *Proc. Natl. Acad. Sci. USA* **100**, 7865–7870.
29. Åkerlund, T., Gullbrand, B. & Nordström, K. (2002) *Microbiology* **148**, 3213–3222.